Solitary death in coupled limit cycle oscillators with higher-order interactions

Subhasanket Dutta, Umesh Kumar Verma, and Sarika Jalan ©*

Complex Systems Lab, Department of Physics, Indian Institute of Technology Indore, Khandwa Road, Simrol, Indore-453552, India

Coupled limit cycle oscillators with pairwise interactions are known to depict phase transitions from an oscillatory state to amplitude or oscillation death. This Research Letter introduces a scheme to incorporate higher-order interactions which cannot be decomposed into pairwise interactions and investigates the dynamical evolution of Stuart-Landau oscillators under the impression of such a coupling. We discover an oscillator death state through a first-order (explosive) phase transition in which a single, coupling-dependent stable death state away from the origin exists in isolation without being accompanied by any other stable state usually existing for pairwise couplings. We call such a state a solitary death state. Contrary to widespread subcritical Hopf bifurcation, here we report homoclinic bifurcation as an origin of the explosive death state. Moreover, this explosive transition to the death state is preceded by a surge in amplitude and followed by a revival of the oscillations. The analytical value of the critical coupling strength for the solitary death state agrees with the simulation results. Finally, we point out the resemblance of the results with different dynamical states associated with epileptic seizures.

a. Introduction. The suppression of oscillations in dynamical systems has been an area of persistent interest due to its occurrence in a wide range of real-world dynamical systems such as climate [1], lasers [2], electronic circuits [3], cell differentiation [4], etc. Quenching of oscillations in large-scale dynamical systems made of interacting units arises primarily from the coupling between these units. For instance, in lasers, a few specific forms of the couplings among the laser components can lead to the quenching of oscillations [2]. In neurological systems, oscillation death has been proposed to be an important root cause of various neurodegenerative diseases and has been modeled using coupled nonlinear oscillators [5,6]. Coupled Stuart-Landau (SL) oscillators provide a prototype model to fathom the origin of oscillator death and associated changes in the stability properties. Earlier investigations on coupled SL oscillators trace a variety of reasons behind the oscillation quenching, such as time delay [7], conjugate coupling [8–10], dynamical coupling [11], or frequency mismatch [12], factors causing a damping effect on the oscillations. Prasad *et al.* observed that for a system of Hindmarsh-Rose neuron oscillators interacting via nonlinear coupling, a death state can be reached for sufficiently strong coupling strength [13]. A death state of an oscillator can be classified into two major categories, amplitude death (AD) and oscillation death (OD), based on the spatial position and symmetry of the associated fixed points. The AD state corresponds to all the oscillators settling down to the same fixed point, which is the unstable fixed point of the uncoupled oscillator. A coupled system stabilizes the AD through Hopf bifurcation while preserving the parity symmetry [5,14]. In contrast, in the OD state, oscillators settle at different fixed

points which originate due to coupling and parity-symmetry-breaking bifurcation [15]. Furthermore, there could be two different routes from the oscillatory state to the oscillation death state: a smooth second-order transition [6,12,16] or an abrupt first-order jump [17,18]. Oscillator death is desired in many real-world systems having unwanted oscillations. For example, instability in the signals of laser systems can be regulated via the amplitude death mechanism [2]. In addition to the quenching, SL oscillators with pairwise couplings have been shown to depict a rich variety of behaviors, such as synchronization [19], chimera, and chimera death [20].

Furthermore, it has increasingly been realized that real-world complex systems made of dynamical units may not only have pairwise interactions but also possess higher-order structures; examples include cliques in the human brain [21], scientific collaborations [22], etc. Studies of coupled Kuramoto oscillators with higher-order interactions have revealed various emerging behaviors, such as infinite multistable synchronized states and phenomena such as abrupt (de)synchronization [23–25]. The Kuramoto oscillator model describes only the phase of a system; however, many real-world complex systems are better described by a model consisting of both amplitude and phase. SL oscillators constitute a limit cycle model which takes into account both factors.

Recently, Carletti *et al.* investigated coupled SL oscillators with linear higher-order interactions on networks [26]. Note that the form of higher-order interactions considered in Ref. [26] gets decomposed into pairwise interactions for globally coupled systems, i.e., in the absence of a network structure. This Research Letter considers coupled SL oscillators with higher-order nonlinear multiplicative coupling which cannot be decomposed into pairwise interactions. We find synchronization, first-order transition to oscillator death, and revival of the oscillations after the death state. A surge in the amplitude of the dynamical variable is accompanied

*sarika@iiti.ac.in

by the synchronization. Importantly, the oscillator death observed here does not get manifested in the pairwise coupled SL oscillators. Usually, the AD state arises when an unstable fixed point of the uncoupled system becomes stable due to the coupling, and the parity symmetry of the system is preserved with an introduction of the coupling; in contrast, the OD state, which corresponds to the birth of more than one fixed point, arises as a consequence of parity symmetry breaking of the uncoupled system due to coupling. This Research Letter reports a state consisting of a single pair of stable and saddle fixed points in SL oscillators upon introduction of the coupling which preserves the parity symmetry. In saddle-node bifurcation, a stable point and a saddle point appear together, where the saddle point has both stable and unstable manifolds. This single stable fixed point arises through the saddle-node bifurcation upon coupling through triadic interactions. The birth of these new fixed points does not change the stability properties of the already existing unstable fixed point of the system. We refer to such a single stable fixed point as a solitary death (SD) state to distinguish it from other coupling-created death states which correspond to the existence of more than one stable fixed point. We perform a linear stability analysis to find the criteria for the occurrence of the SD state. Also, we analyze the basin of attraction of the bistable regions during synchronization, and we analyze the first-order transition to death states and draw bifurcation plots for the coupled system. Finally, we check the robustness of the occurrence of all the phenomena in the presence of change in the value of the intrinsic frequency, introduced pairwise interaction, and nonidentical oscillators in the system.

b. Model. The dynamical equation for an uncoupled SL oscillator can be written as

$$\dot{z}(t) = (a^2 - |z(t)|^2)z + i\omega z.$$

Here, z is a complex variable depicting the dynamical state of an oscillator with ω being its intrinsic frequency. The oscillator has one unstable fixed point acting as a center for a stable circular limit cycle of radius a. We propose a coupling scheme for incorporating higher-order interactions among dynamical units. Our prime consideration while proposing the scheme is that it should not be decomposed into pairwise terms. One of the simplest ways of satisfying this condition is to consider the product of the dynamical states of the interacting oscillators. Moreover, we avoided the conjugate variable z^* in the coupling function since it already yields quenching of the oscillations for pairwise coupling [18]. Hence it will be difficult to assess whether the particular types of oscillation-quenching states reported in this Research Letter arise due to higher-order or conjugate couplings. However, the feedback coupling through z_k in pairwise interaction does not result in quenching. Furthermore, when transformed into polar coordinates, Eq. (1) signifies periodic coupling between the phases of the interacting oscillator, just like the form of higher-order coupling used in the lower-dimensional counterpart (Kuramoto oscillator) [24] of SL oscillators. The coupled dynamical equation is given by

$$\dot{z}_j(t) = (1 - |z_j(t)|^2)z_j + i\omega z_j + \frac{\varepsilon}{N^2}\sum_{k=1}^{N}\sum_{l=1}^{N}z_k z_l. \quad (1)$$

Upon substituting $z_j = r_j e^{i\theta_j}$, we get

$$\dot{r}_j = (1 - r_j^2)r_j + \frac{\varepsilon}{N^2}\sum_{k,l=1}^{N} r_k r_l \cos(\theta_k + \theta_l - \theta_j),$$

$$\dot{\theta}_j = \omega_j + \frac{\varepsilon}{N^2 r_j}\sum_{k,l=1}^{N} r_k r_l \sin(\theta_k + \theta_l - \theta_j),$$

where r and θ are the amplitude and phase of the oscillator, respectively. Upon substituting $z_j = x_j + iy_j$, the resulting equations are

$$\dot{x}_j = P_j^x + \frac{\varepsilon}{N^2}\sum_{k,l=1}^{N}(x_k x_l - y_l y_k),$$

$$\dot{y}_j = P_j^y + \frac{\varepsilon}{N^2}\sum_{k,l=1}^{N}(x_k y_l + x_l y_k),$$

where

$$P_j^x = (1 - x_j^2 - y_j^2)x_j - wy_j,$$
$$P_j^y = (1 - x_j^2 - y_j^2)y_j + wx_j.$$

We further define an order parameter A that quantifies the variance of fluctuation of the dynamical variables over a time span and tends to 0 for the amplitude death. Moreover, to understand phase coherence, we use another order parameter, R, which takes 1 for the synchronized state and 0 for the incoherent state. The order parameters are described by the following equations:

$$A = \frac{1}{N}\sum_{i=1}^{N}(\langle x_i\rangle_{\max,t} - \langle x_i\rangle_{\min,t}), \quad R = \left|\frac{\sum_{i=1}^{N} e^{i\theta_i}}{N}\right|.$$

Here, $\langle x_i\rangle_{\max,t}$ and $\langle x_i\rangle_{\min,t}$ represent the maximum and minimum values, respectively, of x over time t.

c. Different dynamical states. The population of SL oscillators coupled via higher-order interactions [Eq. (1)] is affluent in dynamics and manifests several distinct dynamical states [Fig. 1(a)]. Starting with the initial conditions drawn from a uniform random distribution between 0 and 1 ($x_i(0) \in [0, 1]$, $y_i(0) \in [0, 1] \forall i$), as we increase ε, the system gets synchronized immediately on a limit cycle at a very small value of ε. Upon a further increase in ε, the amplitude of the limit cycle keeps on increasing, and we refer to this state as "enhancement of oscillations" [EO; Fig. 1(b)]. In the forward direction, this state disappears yielding the oscillator death state named "solitary death" (SD) depicted by a 0 value of A at a critical coupling strength ε_{cf} [Fig. 1(c)]. In the backward direction, again starting with a homogeneous distribution for x_i, as ε is decreased adiabatically, initially we encounter a state that oscillates (limit cycle) but is not synchronized and label it as the "revival of oscillations" (RO) state [Fig. 1(d)]. A further decrease in ε yields the SD state, which is finally encountered by a transition to the EO state. However, this transition happens at a lower critical coupling strength than ε_{cf} and is marked as ε_{cb}, thereby giving rise to a hysteresis region. In the following, we describe all these states in detail.

Enhancement of oscillations (EO). The first state we encounter while moving in the forward direction is EO. Here the oscillators are synchronized with the size of the limit cycle increasing with ε. This state disappears at the forward
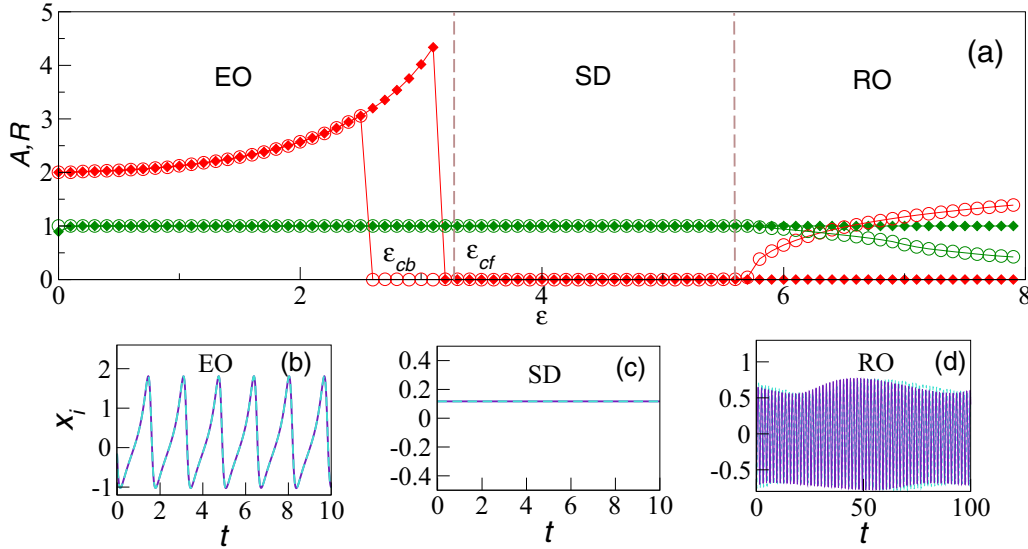
FIG. 1. (a) A, R vs ε and (b)–(d) time series of globally coupled identical SL oscillators [Eq. (1)]: a synchronized state with enhanced oscillation (EO; $\varepsilon = 2.3$) (b), solitary death (SD; $\varepsilon = 3.4$) (c), and a revival of oscillations (RO) state with a toroid ($\varepsilon = 7.5$) (d). Red diamonds (circles) represent A in the forward (backward) direction, and green diamonds (circles) represent R in the forward (backward) direction. Other parameters are $N = 1000$, $\omega = 4.0$, and $x_i(0), y_i(0) \in [0, 1] \, \forall \, i$.

critical point ε_{cf} through a homoclinic bifurcation. For $\varepsilon < \varepsilon_{cb}$ we have the EO state without the existence of the SD state [Fig. 2(a)]; however, at ε_{bf} a pair of points consisting of a stable fixed point and a saddle fixed point are born [Fig. 2(b)]. The saddle point and the stable limit cycle approach each other with increasing ε [Fig. 2(c)] and collide at ε_{cf}, beyond which the limit cycle disappears while the saddle point sur-

vives [Fig. 2(d)]. From ε_{cb} to ε_{cf}, EO shares its basin with the SD state as both the states coexist. Additionally, the backward and forward transition points are different. As illustrated by the bifurcation diagram (Fig. 3), the EO state is depicted in the form of a stable limit cycle whose amplitude increases with ε.

Solitary death (SD) state. Upon a further increase in ε, the system undergoes a first-order transition to the SD state (explosive death). Only one unstable fixed point exists before the critical ε (ε_{cb}). At ε_{cb}, due to the higher-order couplings in the system, a new pair of fixed points is born through the saddle-node (limit point) bifurcation, yielding one stable branch and one unstable branch (Fig. 3). The stable branch corresponds to the solitary death state, and it loses stability when ε increases beyond a certain value. Before that until
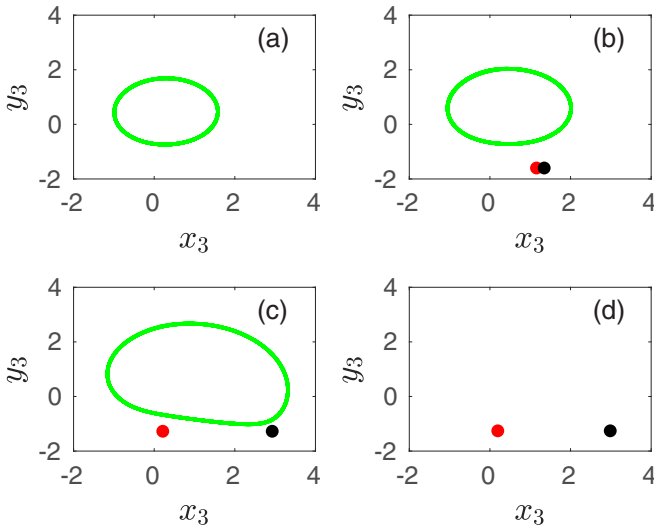

FIG. 2. Coordinate space plot y_3 vs x_3 at various coupling strengths depicting the disappearance of the stable limit cycle via homoclinic bifurcation for SL oscillators [Eq. (1)]. (a) $\varepsilon = 2.0$; existence of the limit cycle. (b) $\varepsilon = 2.51$; birth of a pair of stable and saddle fixed points. (c) $\varepsilon = 3.14$; increase in the amplitude of the limit cycle and approaching the saddle point. (d) $\varepsilon = 3.18$; disappearance of the limit cycle through homoclinic bifurcation. Other parameters are $N = 3$ and $\omega = 4.0$. Solid red and black circles represent the stable fixed point and the saddle fixed point, respectively.
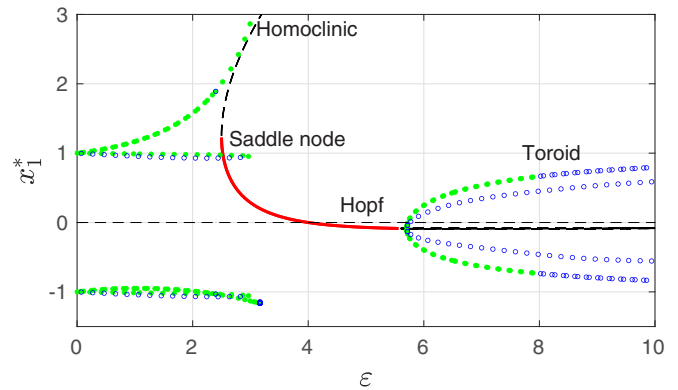

FIG. 3. Bifurcation diagram plotted using XPPAUT [27] for $\omega = 4.0$ and $N = 3$. The stable oscillatory state is depicted by solid green circles, while the unstable oscillatory state is depicted by open blue circles. A stable steady state is represented by the red solid curve, while an unstable steady state is represented by the black dashed curve.

ε_{cf}, this stable fixed point coexists with two other stable limit cycles. This regime is depicted as the hysteresis loop whose width increases with an increase in the value of ω.

The numerical simulations indicate that all the oscillators settle to a common fixed point away from the origin [Fig. 1(c)]. The positions of the fixed points depend on w and k and are given by $(x^{*1} = -\frac{-\omega-2\varepsilon y^*+\sqrt{(\omega+2\varepsilon y^*)^2+4y^*(y^*-y^{*3})}}{2y^*}, \quad y^{*1} = -\frac{\omega}{\varepsilon})$ and $(x^{*2} = \frac{\omega+2\varepsilon y^*+\sqrt{(\omega+2\varepsilon y^*)^2+4y^*(y^*-y^{*3})}}{2y^*}, \quad y^{*2} = -\frac{\omega}{\varepsilon})$ along with the preexisting fixed point $(x^{*3} = 0, y^{*3} = 0)$. Next, the characteristic equation for the Jacobian J, which is a $2N \times 2N$ matrix, can be written in the form

$$|I\lambda - J| = \begin{vmatrix} M_1 + F_1 & \cdot & \cdot & F_1 \\ F_2 & M_2 + F_2 & \cdot & \cdot \\ F_i & \cdot & M_i + F_i & \cdot \\ F_N & \cdot & \cdot & M_N + F_N \end{vmatrix},$$

where $M_1 = M_2 \cdots = M_N = M = \begin{pmatrix} \lambda - 1 + 3x^2 + y^2 & +\omega - 2xy \\ +\omega - 2xy & \lambda - 1 + x^2 + 3y^2 \end{pmatrix}$ and $F_1 = F_2 \cdots = F_N = F = \frac{2\varepsilon}{N}\begin{pmatrix} x & y \\ y & x \end{pmatrix}$. The characteristic equation of these types of solutions is given by [6]

$$\Pi_{i=1}^{N}|M| = 0 \quad \text{and} \quad \left|I_2 + \sum_{i=1}^{N} \frac{\text{adj}(M)F}{|M|}\right| = 0.$$

The fixed point x^{*1} is unstable for all the values of ε and ω, confirming the simulation results. We focus on the following eigenvalues for x^{*2}, y^{*2} to get the stability condition for the SD state:

$$\lambda_{1,2} = 1 - \frac{2\omega^2}{\varepsilon^2} - \frac{\varepsilon^2\eta^2}{2\omega^2} \pm \sqrt{-\omega + \frac{\omega^4}{\varepsilon^4} + \frac{\eta^2}{2} + \frac{\varepsilon^4\eta^4}{16\omega^4}}, \quad (2)$$

$$\lambda_{3,4} = 1 - \frac{2\omega^2}{\varepsilon^2} - \frac{\varepsilon^2\eta}{\omega} - \frac{\varepsilon^2\eta^2}{2\omega^2}$$
$$\pm \sqrt{-\omega + \frac{\omega^4}{\varepsilon^4} + \frac{\eta^2}{2} + \frac{\varepsilon^4\eta^4}{16\omega^4}}, \quad (3)$$

where $\eta = -\omega + \sqrt{\omega^2 - \frac{4\omega}{\varepsilon}(-\frac{\omega}{\varepsilon} + \frac{\omega^3}{\varepsilon^3})}$. The real part of these eigenvalues [Eq. (2)] must be negative for the fixed point to be stable, which provides us with the conditions $\varepsilon < \sqrt{\frac{1+4\omega^2}{2}}$, the upper bound for the stability of the fixed point. Similarly, the lower bound is derived by using the fact that the real part of Eq. (3) is less than zero and consequently $\varepsilon > \sqrt{-2 + 2\sqrt{1+\omega^2}}$. According to these stability conditions, when $\omega = 4.0$, we get $2.5 < \varepsilon < 5.7$, which is in complete agreement with the numerical results (Fig. 4). Upon increasing ω, while both the forward and backward critical coupling strengths corresponding to SD shift towards the right, ε_{cf} shifts much more than ε_{cb}, and consequently, the width of the hysteresis increases. Additionally, the stability region for the SD state also increases with an increase in intrinsic frequency ω. Note that the stability of the SD state is independent of the system size. This helps us to compare the results of numerical simulation ($N = 1000$, Fig. 1) with the bifurcation plot ($N = 3$, Fig. 3) and draw inferences.
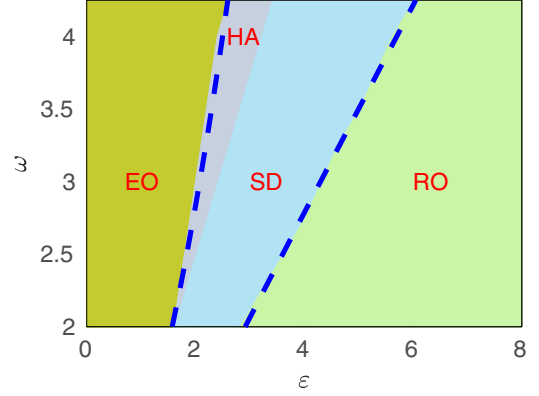

FIG. 4. Phase diagram in the parameter space (ε, ω). The different states are as follows: EO, enhancement of oscillations; HA, hysteresis; SD, solitary death; RO, revival of oscillations. The blue dashed lines are obtained from analytical calculations [Eq. (2)]. The other parameters are $x_i(0), y_i(0) \in [0, 1] \forall i$ and $N = 1000$.

Revival of oscillations (RO). In the forward direction, once a death state is reached, it persists in an increase in ε. In the backward direction, starting from a set of random initial conditions, an oscillatory state is achieved with the decrease in ε. The fixed point corresponding to the SD state does lose its stability at critical ε; however, in the forward direction, we change ε adiabatically, the oscillators stay at the fixed point, and the unstable fixed point keeps getting manifested. In contrast, if we do not set the initial condition corresponding to a fixed point solution (as in the case of the backward direction), an oscillatory state is achieved at critical ε. This state is, however, not simply elliptic in nature; rather it resembles something more like a torus. The bifurcation diagram points out that the stable fixed point loses its stability via Hopf bifurcation yielding an unstable fixed point and a stable limit cycle. This stable limit cycle again loses its stability via toroid bifurcation to become a torus [28]. This torus rotates around an unstable limit cycle as illustrated in the bifurcation diagram (Fig. 3).

d. Sensitivity to initial conditions. As depicted in Fig. 3, for lower ε values, the phase space is shared by two limit cycles. The first one remains as it is with an increase in ε, and the oscillators are not synchronized but are phase locked (PL state). In contrast, in the other branch, the amplitude of the limit cycle (A) increases with ε and corresponds to all oscillators being synchronized (Fig. 1). The system chooses either of the limit cycles to settle based on the initial conditions as evident from the basin plot in Fig. 5(a). Furthermore, in the hysteresis region, depending on the initial conditions, the system goes to the synchronized state or the OD state. Since both the probable states in this region satisfy the condition that $x_i = x_j$ and $y_i = y_j \forall i, j$, we have assumed $x_i = x_j = x_3$ and $y_i = y_j = y_3$ [Fig. 5(b)]. The SD state after $\varepsilon = \varepsilon_{cf}$ does not share its basin with any other state [Fig. 5(c)]. Similarly, in the RO state, if we start the simulations close to the unstable fixed point, the system remains in the SD state; otherwise, it goes to the oscillatory state [Fig. 5(d)].

e. Introduction of pairwise couplings. Next, we add pairwise couplings along with the triadic couplings in the
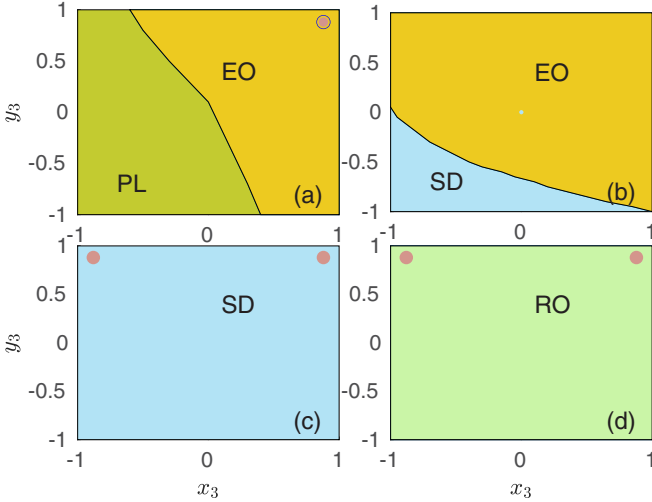
FIG. 5. Basin of attraction for $N = 3$ and $\omega = 4.0$ in Eq. (1). (a) Synchronized state at $\varepsilon = 1.0$, (b) hysteresis at $\varepsilon = 2.7$, (c) solitary death at $\varepsilon = 4.0$, and (d) RO state at $\varepsilon = 7.0$. The different states are as follows: EO, enhancement of oscillations; PL, phase locked; SD, solitary death; RO, revival of oscillations.

following manner:

$$\dot{z}_j(t) = (1 - |z_j(t)|^2)z_j + i\omega z_j + \frac{\varepsilon_p}{N}\sum_{k=1}^{N} z_k$$
$$+ \frac{\varepsilon}{N^2}\sum_{k=1}^{N}\sum_{l=1}^{N} z_k z_l, \qquad (4)$$

where ε_p is the pairwise coupling strength. Figure 6(a) indicates that even for small values of ε_p, synchronization is achieved. Moreover, with the introduction of pairwise couplings, the hysteresis width decreases with an increase in ε_p.

f. Nonidentical coupled oscillators. To gauge the generality of the results presented here, we consider an ensemble of N nonidentical SL oscillators coupled through higher-order as well as pairwise couplings. The dynamics of such a coupled system can be given by

$$\dot{z}_j(t) = (1 - |z_j(t)|^2)z_j + i\omega_j z_j + \frac{\varepsilon_p}{N}\sum_{k=1}^{N} z_k$$
$$+ \frac{\varepsilon}{N^2}\sum_{k=1}^{N}\sum_{l=1}^{N} z_k z_l, \qquad (5)$$

where intrinsic frequencies of SL oscillators are uniformly distributed within $\omega_j \in [4, 5]$. We find that in the absence of pairwise couplings, even for a small spread in the intrinsic frequencies, the system fails to stabilize to a death state [Fig. 6(b)]. In other words, in the absence of pairwise couplings, the death state arising due to higher-order couplings becomes unstable, and the system stays on the same limit cycle even when ε increases. Moreover, at higher ε_p values, both ε_{cb} and ε_{cf} decrease, and so does the hysteresis width.

g. Conclusion. This Research Letter investigates globally coupled identical oscillators with higher-order interactions. We propose a scheme for incorporating higher-order interac-
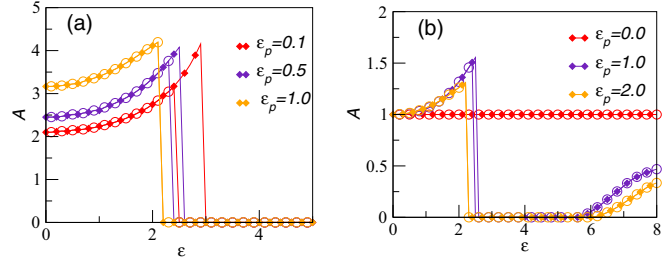

FIG. 6. (a) A vs ε for globally coupled identical SL oscillators having pairwise interactions as well [Eq. (4)] for $\varepsilon_p = 0.1$, $\varepsilon_p = 0.5$, and $\varepsilon_p = 1.0$; $\omega = 4.0$ and $N = 1000$. (b) A vs ε for globally coupled nonidentical SL oscillators [Eq. (5)] for $\varepsilon_p = 0.0$, $\varepsilon_p = 1.0$, and $\varepsilon_p = 2.0$; $\omega \in [4, 5]$ and $N = 1000$. Diamonds, A in the forward direction; circles, A in the backward direction.

tions which cannot be decomposed into lower-order interactions, and the coupled dynamical equation in this scheme also contains a physical meaning in its polar coordinate counterpart. We report the emergence of a coupling-dependent SD state, a single stable quenched state arising from the higher-order interactions. This state might be relevant for real-world complex systems, where a single stabilization point is desired and can be set using the coupling strength. Moreover, incorporation of higher-order interactions yields a first-order transition to death popularly known as explosive death. At lower coupling values the system is usually synchronized along with a surge in the amplitude, and at very high coupling values we observe the SD state transitioning into an RO state in the form of a torus. The surge in the amplitude just after the synchronization resembles the preictal regime in which synchronization is accompanied by an increase in brain activity, which is further followed by a postictal generalized epileptic seizure (PGES) corresponding to a considerable suppression of brain activity [29–31]. These states can be compared with the EO and SD states manifested by Eq. (1). Moreover, at the end of a PGES, the brain might return to a normal state [32] which resembles the RO state discussed here. Furthermore, we calculated the critical coupling strength for occurrence of the SD state using linear stability analysis, which suggested system size independence. Finally, we investigated the dynamical evolution of nonidentical oscillators and found that the nonidentical frequency distribution was responsible for destabilizing the SD state. However, an introduction of the pairwise coupling feedback helped in re-sorting the stability of SD.

This Research Letter only considers triadic couplings to model higher-order interactions. A straightforward extension of the present work is to incorporate other higher-order interactions, such as quadratic and other coupling forms. The effect of network structure on the dynamics of the system could also be an interesting avenue to achieve a more in-depth understanding of how higher-order interactions bring about emerging dynamical features beyond the scope of pairwise interactions.

[1] B. Gallego and P. Cessi, Decadal variability of two oceans and an atmosphere, J. Clim. **14**, 2815 (2001).

[2] M. Kim, R. Roy, J. Aron, T. Carr, and I. Schwartz, Scaling behavior of laser population dynamics with time-delayed coupling: Theory and experiment, Phys. Rev. Lett. **94**, 088101 (2005).

[3] T. Banerjee and D. Ghosh, Experimental observation of a transition from amplitude to oscillation death in coupled oscillators, Phys. Rev. E **89**, 062902 (2014).

[4] A. Koseska, E. Ullner, E. Volkov, J. Kurths, and J. García-Ojalvo, Cooperative differentiation through clustering in multicellular populations, J. Theor. Biol. **263**, 189 (2010).

[5] G. Saxena, A. Prasad, and R. Ramaswamy, Amplitude death: The emergence of stationarity in coupled nonlinear systems, Phys. Rep. **521**, 205 (2012).

[6] S. Dutta, O. Alamoudi, Y. S. Vakilna, S. Pati, and S. Jalan, Oscillation quenching in Stuart-Landau oscillators via dissimilar repulsive coupling, Phys. Rev. Res. **5**, 013074 (2023).

[7] D. V. Ramana Reddy, A. Sen, and G. L. Johnston, Time delay induced death in coupled limit cycle oscillators, Phys. Rev. Lett. **80**, 5109 (1998).

[8] C. Hens, O. Olusola, P. Pal, and S. Dana, Oscillation death in diffusively coupled oscillators by local repulsive link, Phys. Rev. E **88**, 034902 (2013).

[9] J. Wang and W. Zou, Collective behaviors of mean-field coupled Stuart-Landau limit-cycle oscillators under additional repulsive links, Chaos **31**, 073107 (2021).

[10] R. Karnatak, R. Ramaswamy, and A. Prasad, Amplitude death in the absence of time delays in identical coupled oscillators, Phys. Rev. E **76**, 035201(R) (2007).

[11] K. Konishi, Amplitude death induced by dynamic coupling, Phys. Rev. E **68**, 067202 (2003).

[12] A. Koseska, E. Volkov, and J. Kurths, Transition from amplitude to oscillation death via turing bifurcation, Phys. Rev. Lett. **111**, 024103 (2013).

[13] A. Prasad, M. Dhamala, B. M. Adhikari, and R. Ramaswamy, Amplitude death in nonlinear oscillators with nonlinear coupling, Phys. Rev. E **81**, 027201 (2010).

[14] A. Koseska, E. Volkov, and J. Kurths, Oscillation quenching mechanisms: Amplitude vs oscillation death, Phys. Rep. **531**, 173 (2013).

[15] T. Banerjee and D. Ghosh, Transition from amplitude to oscillation death under mean-field diffusive coupling, Phys. Rev. E **89**, 052912 (2014).

[16] R. Mirollo and S. Strogatz, Amplitude death in an array of limit-cycle oscillators, J. Stat. Phys. **60**, 245 (1990).

[17] U. K. Verma, A. Sharma, N. Kamal, and M. D. Shrimali, First order transition to oscillation death through an environment, Phys. Lett. A **382**, 2122 (2018).

[18] K. Sathiyadevi, D. Premraj, T. Banerjee, and M. Lakshmanan, Additional complex conjugate feedback-induced explosive

death and multistabilities, Phys. Rev. E **106**, 024215 (2022).

[19] L. Tumash, E. Panteley, and A. Zakharova, Synchronization patterns in Stuart-Landau networks: A reduced system approach, Eur. Phys. J. B **92**, 100 (2019).

[20] A. Zakharova, M. Kapeller, and E. Schöll, Chimera death: Symmetry breaking in dynamical networks, Phys. Rev. Lett. **112**, 154101 (2014).

[21] A. E. Sizemore, C. Giusti, A. Kahn, J. M. Vettel, R. F. Betzel, and D. S. Bassett, Cliques and cavities in the human connectome, J. Comput. Neurosci. **44**, 115 (2018).

[22] E. Vasilyeva, A. Kozlov, Alfaro-K. Bittner, D. Musatov, A. M. Raigorodskii, M. Perc, and S. Boccaletti, Multilayer representation of collaboration networks with higher-order interactions, Sci. Rep. **11**, 5666 (2021).

[23] T. Tanaka and T. Aoyagi, Multistable attractors in a network of phase oscillators with three-body interactions, Phys. Rev. Lett. **106**, 224101 (2011).

[24] P. S. Skardal and A. Arenas, Abrupt desynchronization and extensive multistability in globally coupled oscillator simplexes, Phys. Rev. Lett. **122**, 248301 (2019).

[25] S. Jalan and A. Suman, Multiple first-order transitions in simplicial complexes on multilayer systems, Phys. Rev. E **106**, 044304 (2022).

[26] T. Carletti, D. Fanelli, and S. Nicoletti, Dynamical systems on hypergraphs, J. Phys.: Complexity **1**, 035006 (2020).

[27] B. Ermentrout, *XPPAUT*, in *Computational Systems Neurobiology* (Springer, New York, 2012), pp. 519–531.

[28] See Supplemental Material at http://link.aps.org/supplemental/10.1103/PhysRevE.108.L062201 for phase space behaviors of different dynamical systems and for results regarding the effect of noise, higher-order interactions with conjugate coupling, and SL oscillators with pairwise interactions, https://github.com/complex-systems-lab/Supplementary-Solitary-death-in-coupled-limit-cycle-oscillators-with-higher-order-interactions.

[29] H. Sohanian Haghighi and A. H. D. Markazi, A new description of epileptic seizures based on dynamic analysis of a thalamocortical model, Sci. Rep. **7**, 13615 (2017).

[30] E. O'Sullivan-Greene, I. Mareels, D. Freestone, L. Kulhmann, and A. Burkitt, A paradigm for epileptic seizure prediction using a coupled oscillator model of the brain, in *2009 Annual International Conference of the IEEE Engineering in Medicine and Biology Society* (IEEE, Piscataway, NJ, 2009), pp. 6428–6431.

[31] V. Grigorovsky, D. Jacobs, V. Breton, U. Tufa, C. Lucasius, J. Campo, Y. Chinvarun, P. Carlen, R. Wennberg, and B. Bardakjian, Delta-gamma phase-amplitude coupling as a biomarker of postictal generalized EEG suppression, Brain Commun. **2**, 11 (2020).

[32] R. S. Fisher and J. J. Engel, Jr., Definition of the postictal state: When does it start and end? Epilepsy Behav. **19**, 100 (2010).